Bioresource Technology 266 (2018) 34–44

Contents lists available at ScienceDirect

Bioresource Technology

journal homepage: www.elsevier.com/locate/biortech

Increased poly-β-hydroxybutyrate production from carbon dioxide in randomly mutated cells of cyanobacterial strain *Synechocystis* sp. PCC 6714: Mutant generation and characterization

Donya Kamravamanesh[a,c], Tamas Kovacs[a], Stefan Pflügl[a,*], Irina Druzhinina[b], Paul Kroll[a,e], Maximilian Lackner[c,d], Christoph Herwig[a,e]

[a] Institute of Chemical, Environmental and Bioscience Engineering, Research Area Biochemical Engineering, Technische Universität Wien, 1060 Vienna, Austria
[b] Institute of Chemical, Environmental and Bioscience Engineering, Research Group for Microbiology and Applied Genomics, Technische Universität Wien, 1060 Vienna, Austria
[c] Lackner Ventures & Consulting GmbH, Hofherr Schrantz Gasse 2, 1210 Vienna, Austria
[d] University of Applied Sciences FH Technikum Wien, 1200 Vienna, Austria
[e] CD Laboratory on Mechanistic and Physiological Methods for Improved Bioprocesses, Technische Universität Wien, 1060 Vienna, Austria

ARTICLE INFO

Keywords:
Poly-β-hydroxybutyrate (PHB)
UV-mutagenesis
Synechocystis sp. PCC 6714
CO_2 uptake rate
Inorganic phosphate system transport (Pst)

ABSTRACT

Photosynthetic Poly-β-hydroxybutyrate (PHB) productivity in cyanobacteria needs to be increased to make cyanobacterial derived bioplastics economically feasible and competitive with petroleum-based plastics. In this study, high PHB yielding mutants of *Synechocystis* sp. PCC 6714 have been generated by random mutagenesis, using UV light as a mutagen. The selection of strains was based on PHB content induced by nitrogen and phosphorus starvation. The fast growing mutant MT_a24 exhibited more than 2.5-fold higher PHB productivity than that of the wild-type, attaining values of 37 ± 4% dry cell weight PHB. The MT_a24 was characterized for phenotypes, CO_2 uptake rate and gene expression levels using quantitative PCR. Genome sequencing showed that UV mutagenesis treatment resulted in a point mutation in the ABC-transport complex, phosphate-specific transport system integral membrane protein A (PstA). The MT_a24 shows potential for industrial production of PHB and also for carbon capture from the atmosphere or point sources.

1. Introduction

Cyanobacteria are promising platforms for the photosynthetic production of poly-β-hydroxybutyrate (PHB) (Oliver et al., 2016). PHB is a promising biotechnological product from the class of bacterial polyhydroxyalkanoates (PHA), which are naturally occurring thermoplastic polyesters and can replace fossil-derived plastics in most applications, such as disposable bulk materials in packaging films, containers, and paper coatings and in biomedical applications (Fabra et al., 2015; Madison and Huisman, 1999). Life cycle assessment studies have suggested that using PHB as a replacement of conventional petrochemical polymers lowers environmental impacts (Pietrini et al., 2007) and also can reduce marine littering and microplastics pollution (Lackner, 2015).

Other than their potential for reducing greenhouse gas emissions and reducing production costs, cyanobacteria have natural pathways for the production of carbohydrates and proteins as well as metabolites such as vitamins and carotenoids (Ruffing and Kallas, 2016; Wang et al., 2014). However, from an economic point of view, photosynthetic PHB production in cyanobacteria has a major drawback, as the native PHB content is normally very low (< 10% dry cell weight (DCW) (Drosg, 2015). Attempts to obtain wild- type high PHB producing cyanobacterial strains have rarely been successful. So far the thermophilic cyanobacterial strain *Synechococcus* sp. MA-19 with 55% (DCW) PHB (Nishioka et al., 2001) is the highest reported amount of PHB from CO_2. Cyanobacterial strain improvement to increase PHB productivity from CO_2 is an important step to enable a feasible production of this biodegradable polymer (Balaji et al., 2013).

Even though the mechanism by which PHB is produced in cyanobacteria is not completely understood, the main accepted hypothesis is that when cyanobacteria are exposed to unfavorable growth conditions, like nitrogen and phosphorus limitation, the excess energy or the disproportion in the ratio of carbon: nitrogen or NADPH: ATP is effectively directed towards carbon reserves such as PHB and glycogen synthesis as

* Corresponding author at: TU Wien, Institute of Chemical, Environmental and Bioscience Engineering, Research Area Biochemical Engineering, Gumpendorfer Straße 1a, 1060 Vienna, Austria.
E-mail address: stefan.pfluegl@tuwien.ac.at (S. Pflügl).

https://doi.org/10.1016/j.biortech.2018.06.057
Received 19 April 2018; Received in revised form 18 June 2018; Accepted 19 June 2018
Available online 20 June 2018
0960-8524/

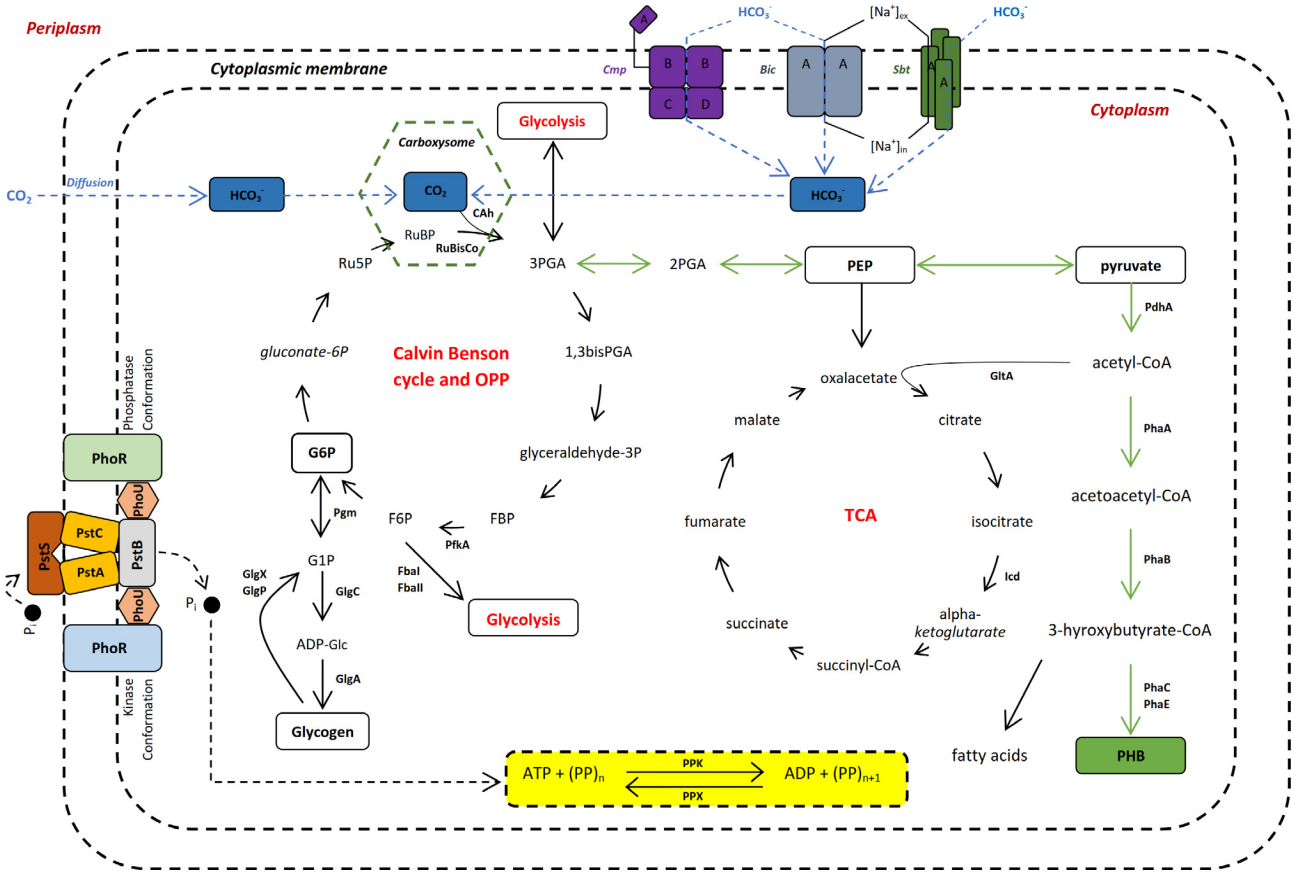

Fig. 1. Simplified biosynthetic pathways for polyhydroxybutyrate (PHB) and glycogen production in cyanobacteria. The pathways are reproduced from the previously shown data by (Burnap et al., 2015; Gao et al., 2012; Vuppada et al., 2018) with some modifications. Two possible routes for the PHB synthesis are shown i) direct carbon dioxide fixation via the Calvin-Benson cycle, producing sugar phosphates and conversion of pyruvate to acetyl-CoA (indicated by green arrows) and ii) via the glycogen oxidation by glycogen catabolic enzymes back to the Calvin-Benson cycle. Not all reactions are given, and the enzymes in Calvin-Benson cycle and tricarboxylic acid (TCA) cycle are not fully shown. **Abbreviations**: Ru5P, ribulose-5- phosphate; RuBP, Ribulose-1,5- bisphosphate; 3PGA, 3-phosphoglyceric acid; 1,3 bisPGA, 1,3-Bisphospho glyceric acid; FBP, Fructose-1,6- bisphosphate; F6P, fructose-6-phosphate; G6P, glucose-6-phosphate; G1P, Glucose-1-phosphate; ADP-Glc, ADP-glucose pyrophosphorylase; OPP, Oxidative Pentose Phosphate pathway; PEP, Phosphoenolpyruvate; pp, polyphosphate; ATP, Adenosine triphosphate; ADP, Adenosine diphosphate; CAh, Carbonic anhydrase. (For interpretation of the references to colour in this figure legend, the reader is referred to the web version of this article.)

reducing equivalents (De Philippis et al., 1992). Cyanobacteria as indicated in Fig. 1 fix atmospheric carbon dioxide via the Calvin-Benson cycle, producing carbon backbones; 3-phosphoglycerate for production of metabolites such as glycogen and PHB in some species (Wang et al., 2013). This metabolite is later utilized to provide the necessary carbon backbone for biosynthesis of proteins and other metabolites required for cell growth when essential nutrients are available (Hauf et al., 2015). PHB is synthesized in three biosynthetic steps where acetoacetyl-CoA is formed from two molecules of acetyl-CoA by the enzyme β-ketothiolase (encoded by *phaA*) (Hauf et al., 2015). In the second step, PhaB (encoded by *phaB*) reduces acetoacetyl-CoA to hydroxybutyryl-CoA, utilizing NADPH as the electron donor (Taroncher-Oldenburg et al., 2000). In the final step of biosynthesis, D-3-hydroxybutyryl-CoA is polymerized to PHB by a PHA synthase, comprising PhaC and PhaE (Hauf et al., 2015; Hein et al., 1998). Efforts to overcome bottlenecks in PHB synthesis pathways, including upregulation of native biosynthetic genes for PHB production namely phaA, B, C and E in *Synechocystis* sp. PCC 6803 in spite of a two-fold higher PHB content (26% DCW) (Khetkorn et al., 2016), could not yield higher productivity in terms of produced PHB per unit of time and reactor volume. Also the heterologous expression of *Cupriavidus necator* (Betaproteobacteria) PHB synthesis genes in *Synechocystis* sp. PCC 6803 (Sudesh et al., 2002) showed an increased activity of PHB synthase but was not associated with a significant increase in PHB levels. Conversely, lower expression of PHB synthesis genes has been reported in genetically engineered *Synechocystis* sp. PCC 6803 with high PHB accumulation (Lau et al., 2014). These observations suggest that PHB synthesis is not only regulated by the levels of enzymes of PHB synthesis, but by other factors such as intracellular metabolite concentrations and redox levels (Dutt and Srivastava, 2017). Since the directed approaches used so far could not lead to successful enhancement of PHB productivity in cyanobacteria, the application of an alternative technique seems crucial.

Mutagenesis, as a substitute approach to genetic engineering, has been used successfully to obtain improved bacterial strains as production hosts in biotechnology (Galanie et al., 2013). Several studies have been carried using microalgae and cyanobacteria to obtain desirable phenotypes using random mutagenesis. Cordero et al. (2011) showed enhancement of leutin production in *Chlorella sorokiniane* (Chlorophyta) by using N-methyl-Ń- nitro-nitrosoguanidine (MNNG) as a mutagen. Also, high triacylglycerol (TAG) yielding mutants of *Nannochloropsis* sp. (Ochrophyta) and *Scenedesmus obliquus* (Clorophyta) were obtained by random mutagenesis approach using ethyl methanesulfonate (EMS) and UV radiation respectively (de Jaeger et al., 2014; Doan and Obbard, 2012). Mutagenesis has also been used to promote phototolerance in the model cyanobacterial strain *Synechocystis* sp. PCC 6803 (Narusaka et al., 1999).

In this current study, the random mutagenesis was used as an effective tool to increase PHB production in the cyanobacterial strain

Synechocystis sp. PCC 6714. The strain can produce up to 16% (DCW) PHB under nitrogen and phosphorous limitation by controlling the process parameters and supply of CO_2 as the only carbon source (Kamravamanesh et al., 2017). The most promising mutants were compared to the wild-type strain in terms of biomass growth and PHB content under defined conditions of a multi-photobioreactor system. BIOLOG Phenotype Microarray (PM) assays were used as a method to check the fitness and to characterize the nitrogen and carbon metabolism in the wild-type strain *Synechocystis* sp. PCC 6714 and the best mutant MT_a24. Genome sequencing and quantitative PCR following mutagenesis were done to get more insight into the PHB accumulation mechanism of cyanobacteria and to define targets for future strain engineering.

2. Material and methods

2.1. Strain and mutant generation

An axenic culture of wild-type strain *Synechocystis* sp. PCC 6714 was purchased from Pasteur Culture Collection of Cyanobacteria (Pasteur Institute, Paris, France). Unless stated otherwise, *Synechocystis* sp. PCC 6714 was grown in BG-11 medium (Rippka et al., 1979) supplemented with 10 mM HEPES buffer pH 8.2 with the addition of 15 g L^{-1} of Kobe agar for plates and 5 mM $NaHCO_3$ as carbon source prior to inoculation. In order to induce nitrogen deficiency, cells were cultured in BG-11 media without nitrate and ammonia. Ferrous ammonium citrate and Co $(NO_3)_2{\cdot}6H_2O$ were substituted with equimolar concentrations of Ferric citrate and $CoCl_2{\cdot}6H_2O$ in terms of iron and copper content. For phosphorus limitation, KH_2PO_4 was replaced with an equimolar concentration of KCl in terms of potassium content.

In total, approximately 10^4 cells from late log phase were plated on agar plates and were incubated at 28± 2 °C under continuous illumination with 50± 5 µmol photon m^{-2} s^{-1} in photosynthetically active radiation (PAR) in an incubator from Infors (Switzerland). Once colonies were visible, the plates were exposed to monochromatic UV light with a wavelength of 254 nm at room temperature. After irradiation, the plates were stored in dark conditions for at least 72 h to reduce light-induced repair mechanisms. Subsequently, the plates were incubated under continuous illumination for 120 h. The mutated colonies were removed from plates and cultivated in liquid media on 6-well plates from Greiner CELLSTAR® (Merk, Austria). After 96 h of incubation, the colonies which showed superior growth when compared to the wild type were screened by measuring OD_{750} using an infinite 200 microplate reader (TECAN, Switzerland). The cells were harvested by centrifugation at 5000*g* at room temperature and were re-suspended in media without nitrogen and phosphorus. The PHB content was determined after 4 and 7 days of limitation. The colonies which showed maximum PHB content after 7 days of limitation were selected for further studies.

2.2. Growth determination and estimation of dry weight

Biomass growth was determined spectrophotometrically at 750 nm using a UV–Vis Spectrophotometer (ThermoFisher Scientific, Waltham, MA, USA) at 24-hour intervals. Dry cell weight (DCW) was determined in triplicates by transferring 10 mL of fermentation broth or shake flask cultures to a reusable pressure filter holder (Sartorius, Göttingen, Germany) and by filtering on a pre-weighed 0.45 µm Cellulose acetate filter paper (Sartorius, Göttingen, Germany) at a pressure of 6 bar for 1 min. Filters were dried overnight at 70 °C and dry weight was determined gravimetrically. A correlation between optical density and DCW could be established, taking into account that this correlation changes over cultivation time and is described in Eq. (1). Cx represents the biomass concentration in g L^{-1}.

$$C_x = 0.37 \times OD_{750} \cdot [g\ L^{-1}] \quad (1)$$

2.3. Bioreactor cultivations

Bioreactor experiments were carried out under sterile conditions in a DASbox Mini Bioreactor System (Eppendorf AG, Hamburg, Germany) with a maximum working volume of 250 mL. The two step cultivations were performed first by allowing the cells to grow on complete BG-11 media for 135 h. The limitation phase started by harvesting the cells using centrifugation at 3000 rpm at room temperature and transferring them back into the reactors containing 250 mL of BG-11 media without nitrogen and phosphorous source. The pH was maintained at 8.5 by addition of 0.5 M HCl or NaOH added to the reactors with a DASGIP MP, multi-pump module (Eppendorf AG, Germany). The agitation was set at 300 rpm and the reactors were bubbled with a mixture of sterile filtered air and 2% CO_2 at a flow rate of 0.4 vvm (6 L h^{-1}). The illumination was done using LED strips wrapped around the reactor vessels providing a light intensity of 60 µmol m^{-2} s^{-1} photons in PAR. The five M18 ports were occupied by pH, DO120 sensor (Hamilton, Reno, NV, USA), OD sensor (Eppendorf DASGIP OD4 Module, 880 nm), and gas inlet and a gas outlet. The exhausted gas was analyzed by a DASGIP GA4 gas sensor module (Eppendorf AG, Hamburg, Germany) with a ZrO_2 sensor for O_2 and infrared CO_2 sensor technology.

All fermentation parameters and variable pump set-points were controlled using the DASware control system (Eppendorf AG, Hamburg, Germany).

Photobioreactor experiments were performed in biological duplicates. Samples were taken in triplicates at 24-hour intervals and were analyzed for dry cell weight, glycogen, and PHB content.

2.4. Determination of glycogen content

Glycogen quantification was done using a protocol from Forchhammer and Tandeau de Marsac (1995) with some modifications. Pre-weighed dried cells from 2 mL culture were heated with 1 mL of 7.5% v/v of the sulfuric acid solution at 95 °C on a heating block (Accublock™, Labnet, USA) for 120 min. Glucose was produced from glycogen by acid hydrolysis, the hydrolysate was then quantified by ion chromatography using the method explained by Hofer et al. (2018). For calibration, pure glycogen (Sigma- Aldrich, USA) was treated accordingly and analyzed in parallel with samples. The method was run on an Ion chromatography ICS-5000 (ThermoFisher Scientific, USA), equipped with a pump (LPG), an autosampler (AS-AP) with a 25 µL sample loop, a detector compartment (DC) and an electrochemical detector. Chromeleon 7.2 was used for the control of the devices as well as for the quantification of the peak areas. The glycogen content per (DCW) was calculated as explained in equation (2).

$$\%\ \text{DCW Gly} = \frac{\text{mg(Gly)}}{\text{mg(DCW)}} * 100. \quad (2)$$

2.5. Determination of the PHB content

PHB quantification was done using the procedure described by Schlebusch and Forchhammer (2010). Pre-weighed dried cells (2–5 mg) were boiled with 1 mL conc. H_2SO_4 at 100 °C on a heating block (Accublock™, Labnet, USA) for one hour to convert PHB to crotonic acid. Samples were allowed to cool down and subsequently diluted 20 times using 0.014 M H_2SO_4. Crotonic acid was determined using a high-performance liquid chromatography system (Thermo-Fischer Scientific, USA) with a Nucleosil C8 column (Macherey-Nagel, Germany) using an isocratic method. The mobile phase used was 20 mM NaH_2PO_4 buffer; pH 2.5 and acetonitrile (70:30 v/v) with a flow rate of 0.85 mL min^{-1} and a column temperature of 30 °C. Detection of crotonic acid was done using a diode array detector (DAD) detector (Thermo-Fischer Scientific, USA) at 210 nm. For calibration, pure PHB (Sigma- Aldrich, USA) was treated accordingly and analyzed in parallel with samples. Instrument

control and peak evaluation were done with Chromeleon 7.2 (Thermo-Fischer Scientific, USA). The percentage PHB per (DCW) was determined by the amount of PHB obtained from HPLC analysis and the cell dry weight of biomass used for the analysis using Eq. (3):

$$\%\text{DCW PHB} = \frac{mg(PHB)}{mg\,(DCW)} * 100. \quad (3)$$

2.6. Phenotyping assay

The phenotyping assay was performed using the Biolog microplates PM1 and PM3B (Biolog, California, USA) for carbon and nitrogen metabolism, respectively. For the carbon assays the cells were suspended into 1:10 diluted BG-11 media with biomass concentration of $OD_{750} = 0.1$. For the nitrogen assays the cells were suspended in BG-11 media with no nitrogen source and 5 mM $NaHCO_3$ as the carbon source. The 90 μL of cell suspension were inoculated into each well and the plates were incubated at 28 °C under 150 rpm agitation and continuous illumination with 30 μmol m^{-2} s^{-1} in PAR in the shaking incubator (Infors, Switzerland). Growth was monitored daily using OD measurements at 750 nm for 168 h, results were analyzed in Statistica 6.0 (StatSoft, USA).

2.7. DNA extraction and genome sequencing

DNA extraction was done for the wild-type strain *Synechocystis* sp. PCC 6714 and the mutant MT_a24 using the DNeasy UltraClean Microbial Kit (QIAGEN, CA, USA) according to the manufacturer's recommendation. The purified DNA pellet was re-suspended in DNase free MQ water, quantified using a Nanodrop 1000 (ThermoFisher Scientific, USA) and stored at −80 °C.

The genome sequencing was done using Illumina Nextera XT libraries on Illumina NextSeq by Microsynth Austria GmbH (Vienna, Austria). The genome was assembled, annotated and the detection of large modifications in the genome was determined using the CLC Genomics Workbench (Qiagen Bioinformatics, CA, USA).

2.8. RNA extraction and quantitative PCR

The cells (25–30 mL) from late exponential phase were harvested by centrifugation at 14000 rpm for 5 min at 0 °C and were stored in liquid nitrogen immediately after sampling. Frozen cells were homogenized in 3 mL lysis buffer, and RNA was isolated using the PureLink RNA Mini Kit (Ambion by life technologies, ThermoFisher Scientific, USA) according to the manufacturer's recommendation. DNA digestion was performed on a column containing RNase-free DNase (On-column DNAase I Digestion Set, Sigma, Austria). The purified RNA pellet was re-suspended in RNase free MQ water and was quantified using a Nanodrop 1000 (ThermoFisher Scientific, USA).

The RNA was reverse transcribed using the RevertAid™ Reverse Transcriptase kit (ThermoFisher Scientific, USA) using 200 ng of total RNA according to manufacturer's protocol with a combination of the provided oligo (dT) and random hexamer primers (20 μL). The quality of the cDNA fragments was analyzed using the Fragment analyzer system (Advanced Analytical Technologies, USA).

Gene expression levels were determined by gene-specific quantitative real-time PCR using Luna Universal qPCR Master Mix (New England Biolabs, USA) and 100 nM primers in the system. The sequences of the forward and reverse primers are provided in (supplementary data). The Cytochrome b6-f complex subunit gene, RNA subunit of ribonuclease P, and a small subunit of ribosomal RNA which maintained constant overall expression (± 20 relative %) both under normal growth conditions and under nitrogen and phosphorus limitation was used as the normalizer. The specification of the PCR was determined using a dissociation stage on a qTower 2.2 (Analytik Jena AG, Germany) system. Determination of primer efficiency was performed using triplicate reactions from a dilution series of cDNA (1, 0.1 and 10^{-2}) for the housekeeping genes mentioned above. For the results, the mean Ct values were determined using the method from (Bustin, 2004) by calculating the average of the triplicate measurements for each species and gene. The ΔCt was calculated by subtracting the mean Ct value of the housekeeping gene from the mean Ct value of the gene of interest. ΔΔCt is constituted by the difference between the mutant sample Ct and the wild-type sample as control Ct values. Finally, the relative quantity, which has been shown in this manuscript was calculated by applying the following equation:

$$\text{Relative quantity} = 2^{-\Delta\Delta Ct} \quad (4)$$

2.9. Statistical analysis

Unless otherwise stated experiments were performed in biological triplicates. Error bars are represented as mean ± standard deviation (SD). Statistical analysis was performed with two tailed Student T-test whereas P values < 0.05 were considered statistically significant.

3. Results and discussion

3.1. Mutant development and screening

Considering strain improvement as a function of growth and PHB production, an accelerated natural evolution approach was used employing UV mutagenesis. At first, the length and distance from the UV light were optimized in terms of viability. Over 2000 mutants were generated after UV irradiation in micro-well plate experiments. All mutants were screened for growth using the wild-type strain *Synechocystis* sp. PCC 6714 as the reference. 850 mutants with superior biomass concentration were further investigated for PHB accumulation. The % DCW PHB content was determined 4 and 7 days after the start of nitrogen and phosphorus limitation using the wild-type strain as a control. In total, 14 mutants showed significantly higher PHB content than the wild-type strain and therefore, were selected for further studies. As shown in Fig. 2 the mutants MT_a16 (31% DCW) and MT_a37 (30% DCW) showed up to 5-fold increase in PHB content compared to

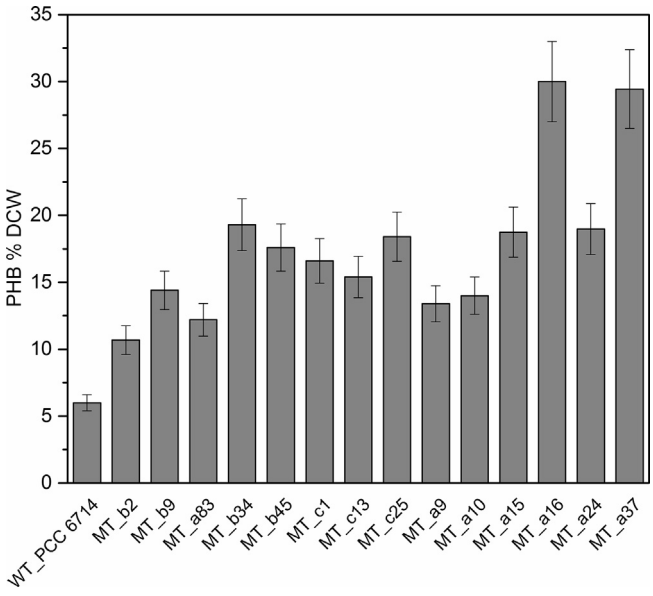

Fig. 2. PHB content of wild-type *Synechocystis* sp. PCC 6714 (WT_PCC 6714) and 14 selected mutants after 7 days of nitrogen and phosphorus limitation. Each data point is obtained from duplicate cultivations and error bars represent mean ± SD.

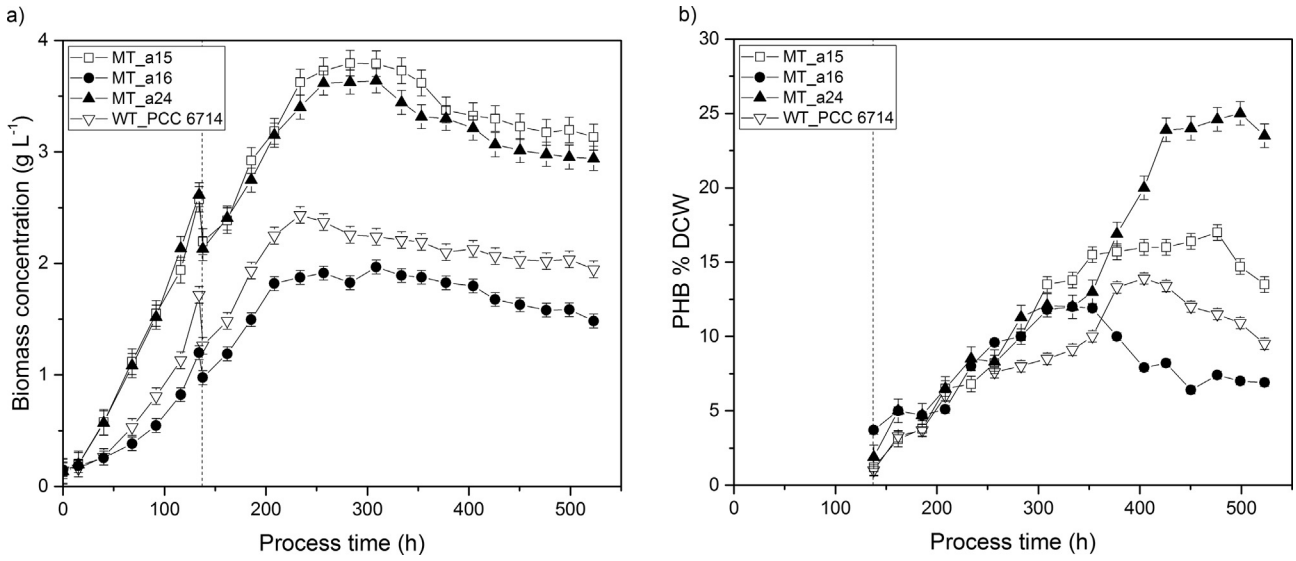

Fig. 3. Two-step cultivation of selected mutants and the wild-type strain *Synechocystis* sp. PCC 6714 in a multi-photobioreactor system a) growth curve for three mutants namely MT-a15, MT_a16, MT_a24 and the wild-type strain *Synechocystis* sp. PCC 6714. b) PHB content in % DCW for the three selected mutants namely MT-a15, MT_a16, MT_a24 and the wild-type PCC6714 strain under nitrogen and phosphorus limitation. The vertical line represents the start of the limitation phase. The values are derived from biological duplicate cultures. Deviation from the duplicate average is indicated by the error bars.

the wild-type *Synechocystis* sp. PCC 6714 with 6% (DCW) PHB after 7 days of nitrogen and phosphorus limitation. Mutants MT_b34, MT_c25, MT_a15 and MT_a24 with 20% (DCW) PHB showed 3.5 folds higher product content when compared to the wild-type. Moreover, as the selection experiments were performed in micro-well plates later during the scale up to shake flask cultivations only three mutants namely, MT_a24, MT_a15 and MT_a16 showed promising potential in terms of biomass growth and PHB production. For instance, the strain MT_a37 showed major defects after multiple cultivations resulting in inferior growth and PHB yield and subsequently was not used for further experiments. To this end, the three mutants MT_a24, MT_a15 and MT_a16 were selected for bioreactor cultivations.

3.2. Mutant characterization

3.2.1. Growth and PHB content

With the view to study growth kinetics and PHB productivity of three selected mutants and the wild-type strain *Synechocystis* sp. PCC 6714, a two-step cultivation was done under controlled defined conditions in a multi-photobioreactor system. The results which are shown in Fig. 3a indicate superior biomass growth for two mutants, namely MT_a24 and MT_a15 both under normal as well as limiting growth conditions when compared to the wild-type. The maximum biomass concentration for mutant MT_a24 was 3.6 ± 0.4 g L^{-1} after 283 h of the process and 3.8 ± 0.4 g L^{-1} for mutant strain MT_a15, which were respectively 1.5 and 1.6 times higher than the wild-type with a maximum biomass concentration of 2.4 ± 0.2 g L^{-1}. The mutant MT_a16 with 2 ± 0.2 g L^{-1} achieved the lowest biomass concentration. The doubling time determined for the mutants MT_a24 and MT_a15 were respectively 16.2 and 16.4 h which are much lower than the doubling times obtained for the mutant MT_a16 and wild-type strain with 40 and 27.9 h. Analysis of the PHB content of the studied strains showed that the highest PHB content of 25 ± 0.7% (DCW) was obtained after 500 h for MT_a24 and 17 ± 0.8% (DCW) for MT_a15 while the wild-type strain reached at 14 ± 0.5% (DCW) PHB after 405 h of nitrogen and phosphorus limitation (Fig. 3b). The maximum polymer concentration was obtained for the mutant MT_a24 with highest PHB content of 735 ± 28 mg L^{-1} after 426 h followed by mutant MT_a15 with 530 ± 20 mg L^{-1} after 476 h. The PHB content obtained for the MT-a24 and MT_a15 were 2.5 and 1.8 times higher, respectively, when compared to that of the wild-type strain. The maximum PHB content for the wild-type strain *Synechocystis* sp. PCC 6714 was 297 ± 15 mg L^{-1} which in turn was higher than that of the mutant MT_a16 with 233 ± 12 mg L^{-1}.

The specific growth rates, average, and maximal volumetric biomass productivity, as well as the volumetric PHB productivity, are shown in Table 1. Under nitrogen and phosphorus replete growth, MT_a24 had the highest average biomass productivity compared to the wild-type and the other two mutants, MT_a15 and MT_a16, with the value of 413 ± 40 mg L^{-1} d^{-1}. However, under nitrogen and phosphorus limiting conditions, MT_a15 showed the highest average biomass productivity of 66 ± 7 mg L^{-1} d^{-1} when compared to the wild-type followed by the MT_a24 with 54 ± 5 mg L^{-1} d^{-1}. The highest maximum volumetric biomass productivity both for growth and limitation phase was obtained for the MT_a15 with 636 ± 64 mg L^{-1} d^{-1} and 537 ± 54 mg L^{-1} d^{-1} respectively. Also, the MT_a24 and MT_a15 obtained the highest average specific growth rate of 0.5 d^{-1}. However, the maximum specific growth rate was slightly higher for mutant MT_a24 than MT_a15 with values of 1.07 and 1.05 d^{-1} which are one and half-fold higher than for the wild-type strain with a maximum specific growth rate of 0.7 d^{-1}. The highest average volumetric PHB productivity was obtained for mutant MT_a24 with the value of 36.9 ± 4 mg L^{-1} d^{-1} which was at least three-fold higher than that of the wild-type strain with 11 ± 1 mg L^{-1} d^{-1}. The highest maximum volumetric PHB productivity was obtained respectively for MT_a15 with 173.7 ± 17 mg L^{-1} d^{-1} and MT_a24 with 134.2 ± 13 mg L^{-1} d^{-1}.

3.2.2. Carbon uptake rate and the link to PHB productivity

The earlier results showed superior volumetric biomass and PHB production for two mutant strains of *Synechocystis* sp. PCC 6714, MT_a15 and MT_a24. These observations encouraged the determination of CO_2 uptake rate and the possible correlation to PHB production. As it could be expected the higher net CO_2 consumption was obtained for mutants MT_a24 followed by the MT_a15 with values of 1140 and 900 mmol, respectively (Fig. 4a). These values are 4 and 3 fold higher, respectively than the values obtained for the wild-type (277 mmol) and the mutant MT_a16 (238 mmol). In order to evaluate whether the higher CO_2 consumption in MT_a24 and MT_a15 was due to higher biomass concentration or other unknown genetic or metabolic

Table 1
Volumetric productivities and the specific growth rates of *Synechocystis* sp. PCC 6714 and three selected mutants. The maximum specific growth rate is given as the highest value observed between two daily sampling points. The average and the maximum specific growth rates shown were only determined for the growth phase (0 – 135 h). The average productivities are calculated as the amount of biomass and PHB formed over the course of time per liter of culture media. The maximal productivities represent the highest production values between two consecutive time points. Data represent mean ± SD of biological duplicate cultures. Bold numbers represent the highest number for each parameter.

Strain	Media	Volumetric biomass productivity mg L^{-1} d^{-1}		Specific growth rate d^{-1}		Volumetric PHB productivity mg L^{-1} d^{-1}	
		Average	Maximum	Average	Maximum	Average	Maximum
WT_PCC 6714	N^+P^+	262 ± 30	588 ± 60	0.41	0.70		
	N^-P^-	15 ± 1	451 ± 45			11.0 ± 1	101.6 ± 10
MT_a24	N^+P^+	**413 ± 40**	618 ± 60	**0.50**	**1.07**		
	N^-P^-	54 ± 5	401 ± 40			**36.9 ± 4**	134.2 ± 13
MT_a15	N^+P^+	406 ± 40	**636 ± 64**	**0.50**	1.05		
	N^-P^-	**66 ± 7**	**537 ± 54**			26.4 ± 3	**173.7 ± 17**
MT_a16	N^+P^+	170 ± 17	377 ± 38	0.35	0.41		
	N^-P^-	40 ± 5	323 ± 32			7.14 ± 0.7	84.6 ± 8

The N^+P^+ represents growth when sufficient media components were available (growth phase, first 135 h of the cultivation)
The N^-P^- represents growth under nitrogen and phosphorous limiting conditions (from 135 h until the end of the cultivation).

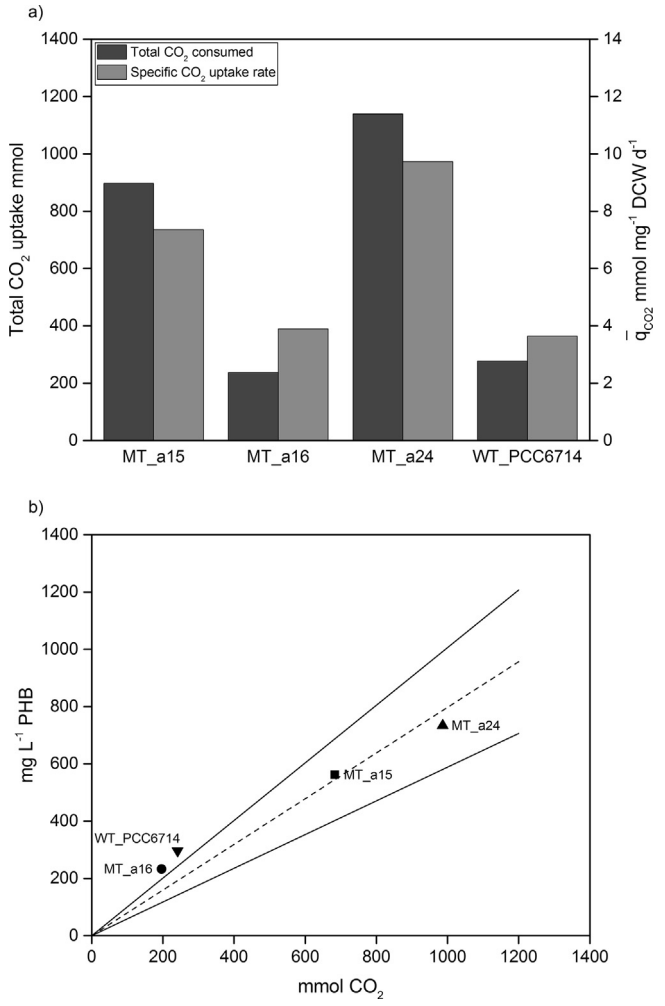

Fig. 4. The net consumed CO_2 (in mmol), the average specific CO_2 uptake rate and correlation to PHB formation are shown. (a) The total net CO_2 consumed and the average specific CO_2 uptake rate in mmol CO_2 mg^{-1} DCW d^{-1} are shown for three mutants MT_a15, MT_a16, MT_a24, and the wild-type strain *Synechocystis* sp. PCC 6714. (b) The results of the linear regression analysis of net CO_2 consumption and maximum PHB produced are shown for a two-step cultivation. The model obtained shows statistically significant parameters with the coefficient of determination, $R^2 = 0.98$ and p value of 0.001 with an upper and lower 95% limit of 1.0 and 0.59, respectively. The experiments were done in biological duplicate cultures and one cultivation is shown as an example.

alterations, the specific CO_2 uptake rate was determined in mmol CO_2 consumed per mg biomass generated per day. Besides net CO_2 consumption, the average specific uptake rates of CO_2 are higher for the mutants with higher PHB productivity namely MT_a24 (9.7 mmol mg^{-1} d^{-1}) and MT_a15 (7.4 mmol mg^{-1} d^{-1}) compared to the WT_PCC 6714 (3.7 mmol mg^{-1} d^{-1}) and MT_a16 (3.8 mmol mg^{-1} d^{-1}) (Fig. 4a). In order to correlate CO_2 uptake of the respective strain with PHB production, linear regression analysis was performed using the highest PHB content obtained for each individual strain during limitation phase and the CO_2 consumed up to that time point. As shown in Fig. 4b the CO_2 uptake directly correlates with PHB production for the two strains MT_a24 and MT_a15. Strains MT_a16 and PCC 6714 are out of 95% interval showing slightly lower CO_2 consumption than the amount of PHB which was produced which could be due to differences in PHB yield or simply other unknown mechanisms. The slope of the linear regression line in Fig. 4b represents the product yield $Y_{PHB/CO2}$, which is 0.80 ± 0.21. The data obtained here are consistent with our previous observations. The mutant MT_a24 shows superior volumetric biomass and PHB productivity, as well as higher specific CO_2 uptake rate compared to the other mutants and the wild-type strain. Hence, mutant MT_a24 was used hereafter for detailed examination and further experiments.

3.2.3. Phenotyping Microarray

The ultimate goal in biotechnological strain improvement is to obtain desirable phenotypes such as high productivity. As a result of random mutagenesis in MT_a24, the volumetric productivities and CO_2 uptake rate were increased. Hence, evaluation of the effect of the mutation on carbon and nitrogen assimilation behavior was performed. Therefore, the mutant MT_a24 was compared to its parent, wild-type strain *Synechocystis* sp. PCC 6714 using carbon and nitrogen Biolog PM assays. The Biolog PM assay has been used for metabolic phenotyping of various microbial species including bacteria, fungi and also microalgae (Pinzari et al., 2016). However, it has not been reported for the phenotyping of cyanobacteria. The complete growth curve was generated for each nutrient source. Table 2 shows the maximum specific growth rate and the average biomass concentration for statistically significant nitrogen and carbon sources after 144 h of cultivation where the difference in OD_{750nm} of the wild-type and mutant MT_a24 was higher than 0.15 and the p values < 0.05. In general, under normal growth conditions when nitrate was used as nitrogen source the MT_a24 grew similar or superior to the wild-type on most carbon sources. The best carbon sources for the growth of MT_a24 were D-Pscicose and glycyl-L-glutamic acid with an OD_{750nm} of 0.53 and 0.54, respectively. The best nitrogen sources for the MT_a24 were identified to be nitrate

Table 2
Average biomass growth on statistically significant carbon and nitrogen sources from Biolog PM Assays. The average biomass concentration (OD_{750}) and maximum specific growth rate (μ_{max}) are given for the statistically significant carbon and nitrogen sources for wild-type strain *Synechocystis* sp. PCC 6714 (1) and the best mutant MT_a24 (2). The standard deviation and P values are given. The carbon and nitrogen sources which have significantly higher growth in mutant MT_a24 are given in bold.

WT_ PCC 6714 = 1 MT_a24 = 2	1 $\mu_{max}(d^{-1})$	1 Average biomass conc. OD_{750}	1 SD	2 $\mu_{max}(d^{-1})$	2 Average biomass conc. OD_{750}	2 SD	P value
Carbon sources							
Glycyl-L-glutamic acid	0.048	**0.34**	0.03	**0.240**	**0.54**	0.18	0.002
Glycin-L-proline	0.024	0.25	0.01	0.048	0.34	0.03	0.001
Phenylethylamine	0.024	0.17	0.02	0.072	0.26	0.05	0.007
Inosine	0.024	0.24	0.01	0.024	0.34	0.02	< 0.001
D-glucose-1-phosphate	0.024	0.26	0.02	0.072	0.41	0.10	0.011
D-glucose-6- phosphate	0.024	0.20	0.02	0.168	0.29	0.12	< 0.001
N-acetyl-D-glucosamine	0.004	0.15	0.01	0.048	0.23	0.05	0.011
L-arabinose	0.024	0.12	0.04	0.048	0.18	0.02	0.016
D-Pscicose	**0.072**	**0.35**	0.10	**0.192**	**0.53**	0.11	0.028
Bromo succinic acid	0.024	0.26	0.01	0.120	0.46	0.10	0.008
Propionic acid	0.024	0.23	0.01	0.024	0.25	0.03	< 0.001
D-gluconic acid	0.005	0.15	0.01	0.072	0.23	0.06	< 0.001
m- tartaric acid	**0.003**	0.20	0.07	0.192	0.30	0.05	0.025
m- hydroxy phenyl acetic acid	0.024	0.29	0.04	0.096	0.37	0.08	0.044
D- galacturonic acid	0.024	0.15	0.02	0.096	0.27	0.07	0.004
Control (No carbon source)	< 0.001	0.12	0.01	0.001	0.16	0.01	0.001
Nitrogen sources							
Nitrite	0.048	**0.18**	0.07	**0.216**	**0.40**	0.18	0.036
Nitrate	**0.072**	0.18	0.07	0.096	0.32	0.11	0.039
Control (No nitrogen source)	< 0.001	0.08	0.01	0.001	0.11	0.01	0.004

Maximum specific growth rate and the average biomass concentration were determined for statistically significant nitrogen and carbon sources after 144 h of cultivation where the difference in OD_{750nm} between the wild-type and mutant MT_a24 was higher than 0.15, corresponding to a p value of < 0.05.

and nitrite with maximum OD_{750nm} of 0.40 and 0.32, respectively. For the mutant MT_a24, rapid growth, as well as the ability to assimilate diverse substrates as carbon and nitrogen source, is a great advantage as it suggests a high degree of fitness of the strain.

3.2.4. Stability of the mutation

The mutant MT_a24 generated in this study was regularly screened for the stability of the mutation over multiple generations, as the mutant does not contain a selection marker or any other trait to apply an external selection pressure to maintain the mutation. The results obtained from four individual two-step cultivations of MT_a24 over the course of 500 h is presented in Fig. 5. The biomass growth curves displayed in Fig. 5a shows that the maximum volumetric biomass concentration obtained for all cultivations was 4.6 ± 0.2 g L^{-1}. A similar pattern for growth has been observed both during growth and limitation of nitrogen and phosphorus. For all the cultivations of MT_a24, PHB and glycogen were accumulated simultaneously during the beginning of the limitation phase. The glycogen content reached a maximum of 50 ± 2% (DCW) after 73 h of nitrogen and phosphorous limitation (200 h from the start of the process) (Fig. 5b and c). Glycogen levels started to decline once the maximum level was reached while PHB content increased further to a maximum of 37 ± 4% (DCW) after approximately 450 h of cultivation (14 days of nitrogen and phosphorus limitation). The data obtained show the stability of the mutant MT_a24 over the course of 10 months. The strain MT_a24 was therefore deposited at National Collection of Microorganisms Cultures (CNCM)-Pasteur Institute (Paris, France) with the registration number (I-5255).

3.3. Genome sequencing and quantitative real-time PCR

3.3.1. Genome sequencing

The mutant strains were selected after physical mutagenesis solely based on improved product formation, while the biochemical or genetic nature of the mutation remained unknown. In order to elucidate the genetic basis causing the superior phenotype of strain MT_a24, whole genome sequencing of both mutant MT_a24 as well as wild-type *Synechocystis* sp. PCC 6714 used for the mutation experiments was performed. The sequence of the reads was mapped to the published genome of *Synechocystis* sp. PCC 6714 (Kopf et al., 2014). The sequenced genome of the mutant MT_a24 was deposited at National Center for Biotechnology Information with the accession number (SRP149881). A comparison of the two sequenced strains *Synechocystis* sp. PCC 6714 wild-type strain and mutant MT_a24 showed that surprisingly, only one mutation causing an amino acid substitution was introduced into the genome of MT_a24. The single mutation was found in an ABC transporter system, exhibited in (Supplementary data). The missense mutation which has resulted in the substitution of a single amino acid alanine (A) to proline (P) is located in the *PstA* gene from the inorganic phosphate-specific transport system (Pst). The Pst system constitutes of a periplasmic inorganic phosphate (P_i)- binding protein (PstS), two integral inner membrane proteins (PstA and PstC) that form a transmembrane channel which transport Pi through the cytoplasmic membrane, and an ATP-binding protein (PstB) (Surin et al., 1985). Besides transporting phosphate, the Pst system plays an important role in the regulation of a number of coordinately regulated genes that are phosphate repressible, of which the best known is *phoA*, the structural gene for alkaline phosphatase (Bachmann, 1983). The *pstA* gene encodes an integral membrane protein with six transmembrane helices (Surin et al., 1985), and its interruption reduces Pi transport, most likely by reducing the affinity of the protein and, hence, the Pst system, for insertion of P_i into the membrane (Rao and Torriani, 1990). Two copies of Pst systems, known as Pst1 and Pst2, have been identified in the genome of the cyanobacterial strain *Synechocystis* sp. PCC 6803 (Burut-Archanai et al., 2011). Both Pst systems encode ABC transporters and are upregulated during phosphate limiting conditions (Burut-Archanai et al., 2011). A mutation in Pst genes blocks Pi uptake under Pi-limited conditions (Cox et al., 1981). This may suggest a different level of phosphate transportation for the mutated strain MT_a24. To that end, the intracellular polyphosphate (PolyP) concentration of the wild-type strain *Synechocystis* sp. PCC 6714 and MT_a24 was analyzed using inductively coupled plasma optical emission spectroscopy (ICP-OES). It has been shown that microorganisms store phosphorus in the form of PolyP when it is provided in excess (Rao et al., 2009). The PolyP storage form provides supplementary source of ATP when not enough

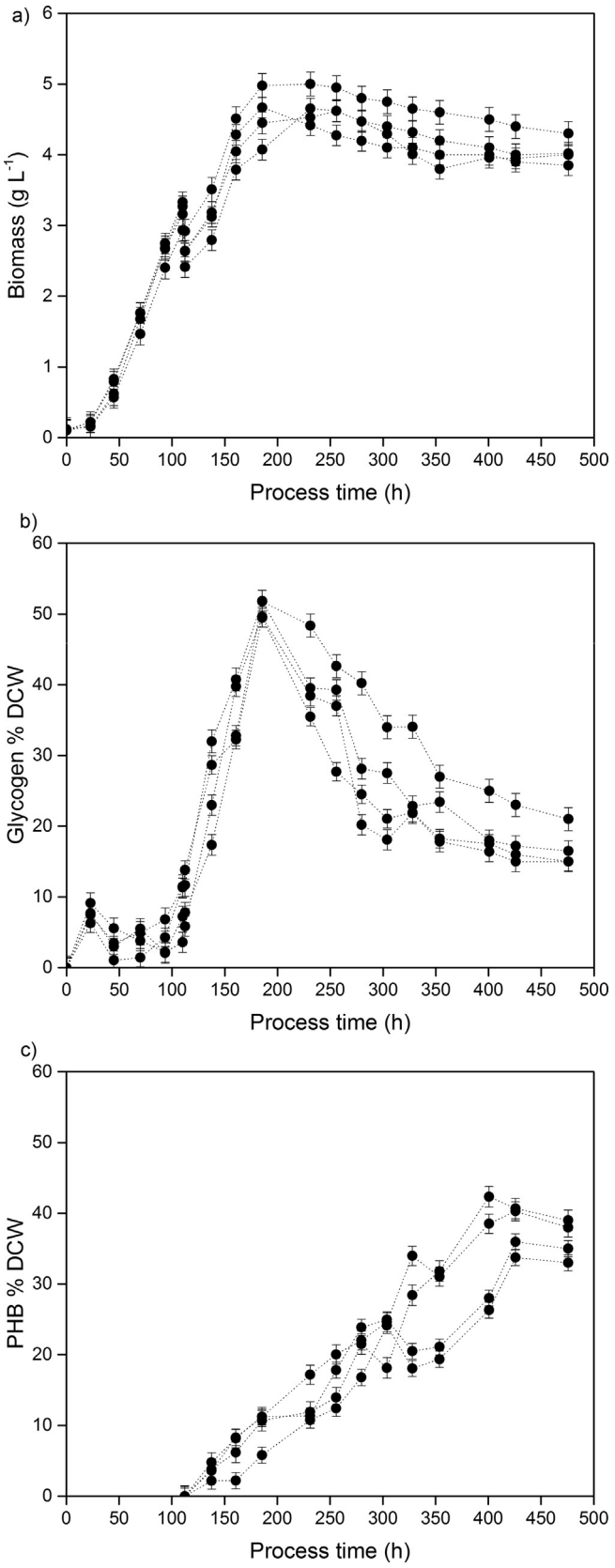

Fig.5. The mutant stability analysis using quadruplicate cultivations. (a) Biomass growth curves (b) percentage DCW glycogen content and (c) percentage DCW PHB content is shown for the quadruplicate cultivation of MT_a24 using a two-step process. The limitation of nitrogen and phosphorus was started at 115 h of the process. Data represent mean ± SD from three independent measurements.

ATP is produced by photosynthesis (Gomez-Garcia et al., 2013).

Surprisingly, the intracellular phosphorus concentrations showed similar levels for the mutant MT_a24 and the wild-type strain. For the sake of gaining insight into the gene expression levels of MT_a24 in comparison to the wild-type strain quantitative real-time PCR was performed for growth and nitrogen and phosphorus limiting conditions.

3.3.2. Quantitative real-time PCR

To study the effect of the mutation on gene regulation, quantitative real-time PCR analysis was performed checking the gene expression levels for the mutant MT_a24 and the parent strain *Synechocystis* sp. PCC 6714 during nitrogen and phosphorus limiting conditions. For the qPCR analysis of the wild-type strain *Synechocystis* sp. PCC 6714 and MT_a24 the genes involved in PHA biosynthesis, glycogen metabolism, bicarbonate, and phosphate transport system, as well as polyphosphate metabolism, were investigated. The analysis was performed on samples derived from 4 and 9 days of limitation. The relative expression levels of the studied genes after 9 days of nitrogen and phosphorus limitation are presented in Fig. 6. As a result of the mutation the expression level of eight genes, namely glycogen phosphorylase (*glgP*) (*p value = 0.045*), Bicarbonate transport system permease protein (*cmpB*) (*p value = 0.035*), bicarbonate binding protein (*cmpA*) (*p value = 0.040*), bicarbonate transport ATP-binding protein (*cmpC*) (*p value = 0.035*), large subunit of RuBisCO (*rbcL*) (*p value = 0.029*), exopolyphosphatase (*ppx*) (*p value = 0.050*), phosphoglucomutase (*pgm*) (*p value = 0.032*) and phosphate transporter protein C (*pstC*) (*p value = 0.043*) was increased in MT_a24 under nitrogen and phosphorus limiting conditions.

Upregulation of genes involved in bicarbonate transportation (*cmpA*, *cmpB*, *cmpC* and *sbtA*) was detected. This observation along with higher expression levels for *rbcL* supports our earlier results which have shown the superiority of mutant MT_a24 in terms of CO_2 uptake. The expression levels for PHA biosynthetic genes (*phaA*, *phaB*, *phaC,* and *phaE*) remain largely unchanged for the MT_a24 when compared to the wild-type strain. However, for the glycogen metabolic genes, namely glycogen phosphorylase (*glgP)* and phosphoglucomutase (*pgm*) expression levels exceeded those of the parental wild-type (WT- PCC 6714) under nitrogen and phosphorus limiting conditions.

In cyanobacteria the glycogen biosynthesis occurs via the phosphoglucomutase (Pgm) which catalyzes the first step of the interconversion of glucose-6P into glucose-1P, followed by the action of ADP-glucose pyrophosphorylase (GlgC) that synthesizes ADP-glucose, using glucose-1P and ATP (Diaz-Troya et al., 2014; Xu et al., 2013). This reaction generates PPi, which is converted into phosphate by a soluble pyrophosphatase (Diaz-Troya et al., 2014). The glycogen synthase (GlgA), later transfers the glucose moiety of the ADP-glucose to the non-reducing end of a linear α-1, 4 glucan. At the end, the glycogen branching enzyme (GlgB) adds α-1, 6 glycosidic bonds synthesizing glycogen branches (Diaz-Troya et al., 2014; Suzuki et al., 2010; Xu et al., 2013). As the nitrogen limitation persists, stored glycogen is oxidized by glycogen catabolic enzymes such as glycogen phosphorylase (encoded by *glgP*) or isoamylases (encoded by *glgX*) (Osanai et al., 2007). Therefore higher expression levels of *glgP* may suggest higher glycogen catabolic activity. As a result, more glucose-1P is converted back into glucose-6P by pgm which is then further catabolized via glycolysis to pyruvate and then through acetyl-CoA to PHB (Osanai et al., 2005). The upregulation of exopolyphosphatases (*ppx*) in the MT_a24 compared to the wild-type PCC 6714 may indicate a higher activity of the enzyme to produce phosphorus from polyphosphate (PolyP). PolyP is synthesized in bacteria from ATP by polyphosphate kinase 1 (PPK1, encoded by *ppk*) and is degraded by exopolyphosphatases (*ppx*), a recessive enzyme which releases the terminal P_i from long-chain linear PolyP (Akiyama et al., 1993). During growth phase and the 4 days of limitation of phosphate, MT_a24 shows upregulation of *ppk* (data not shown) which in turn suggests higher PolyP synthesis activity. As the limitation persists, 9 days of nitrogen and phosphorus limitation, *ppx* is upregulated. Meaning that PolyP is being degraded to

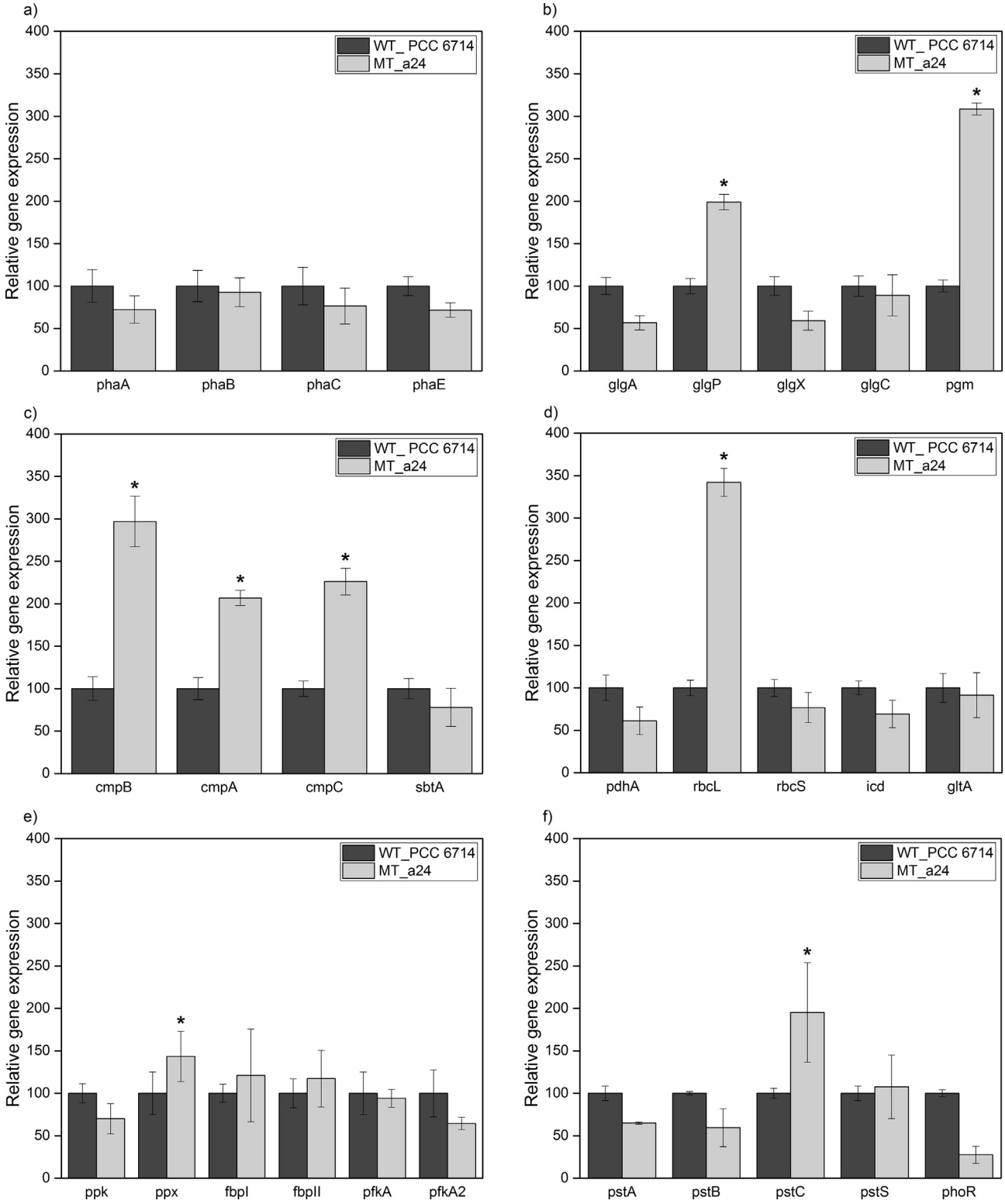

Fig. 6. Quantitative real-time PCR analysis of the wild-type and mutant MT_a24 strain. The relative expression levels of genes involved in (a) PHA biosynthesis (*phaA*, *phaB*, *phaC*, *phaE*), (b) glycogen metabolism (*glgA*, *glgP*, *glgX*, *glgC, pgm*) (c) bicarbonate transportation system (*cmpA*, *cmpB*, *cmpC* and *sbtA*) (d) Rubisco (*rbcL* and *rbcS*), TCA cycle (*pdhA*, *gltA* and *icd*) (e) polyphosphate metabolism (*ppk*, *ppx*, *fbpI*,*fbpII*, *pfkA* and *pfkA2*) and (f) phosphate transport system (*pstA*, *pstC*, *pstB*, *pstS* and *phoR*) are shown. Data represent mean ± SD from three independent observations. Statistical analysis was performed using two tailed Student T-test whereas p values < 0.05 were considered statistically significant shown with *. Levels were calibrated relative to that of the wild-type strain *Synechocystis* sp. PCC 6714 under nitrogen and phosphorus limiting conditions (set as 100%).

provide P_i for metabolic and cellular activities, e.g. as a precursor of ATP synthesis.

The evaluation of expression levels of genes responsible for inorganic phosphate transportation indicates upregulation of *pstC* and downregulation of *pstA* and *pstB*. The phosphate regulon sensor histidine kinase (PhoR) which is involved in the phosphorylation of PhoB in

response to environmental signals (Vuppada et al., 2018) was also shown to be downregulated by three-fold. This result along with the previous information obtained from genome sequencing may indicate that the mutation has resulted in a lower activity of the PstA transport channel resulting in a potentially higher activity of PstC indicated by upregulation of *pstC*. Yet not every data obtained could successfully link the genotypes observed for MT_a24 to the superior phenotypes. We hypothesize that maybe imbalanced phosphate transportation is the cause of change in metabolism of MT_a24. One can confirm this by inserting the Pst genes of the MT_a24 into the wild-type strain *Synechocystis* sp. PCC 6714. It has been shown by Monds et al. (2001) that mutations of *pstC* and *pstA* genes of the phosphate-specific transport operon can cause severe phenotypic changes in organisms such as loss of the ability to form biofilms by *Pseudomonas aureofaciens* PA147-2. This report along with our observations propose a more detailed investigation as well as identification of the functional role of genes involved in phosphate transportation in cyanobacteria.

The main goal of this current study was to increase the PHB productivity by random mutagenesis in cyanobacteria to make photosynthetic PHB production competitive with conventional fossil-based polymers. The mutant MT_a24 generated by UV mutagenesis in this study showed more than 2.5-fold higher PHB content under nitrogen and phosphorus limitation compared to that of the wild-type strain *Synechocystis* sp. PCC 6714 from CO_2. Besides the increase in PHB content, superior biomass productivity, higher specific growth rates, and better fitness was also obtained for MT_a24. Therefore, MT_a24 should be considered as a potential strain for PHB production, since the increased PHB productivity brings economical sensibility to cyanobacterial biopolymer production.

4. Conclusions

This study resulted in the characterization of the mutation in the genome of the MT_a24 strain of *Synechocystis* sp. PCC 6714, however, there is much more to explore in this interesting improved cyanobacterium. It would be of great interest to study the influence of phosphate on metabolic pathways and explore its actual role in PHB biosynthesis of cyanobacteria in the future. The results from this work provide clear evidence that the random mutagenesis approach can help identify target genes for future genetic engineering in cyanobacteria.

5. Declaration of conflict of interest

None.

Acknowledgments

The authors would like to thank Christoph Slouka and Alexandra Hofer for critical reading of the manuscript and preparation of the art work presented.

Authors contributions

DK and SP planned the experiments for mutant generation, selection, and characterization and the bioreactor cultivations. DK performed the experiments, analyzed the data and wrote this manuscript. TK and SP designed the primers and planned qPCR experiments. TK and DK performed the quantitative PCR experiments and the data analysis. SP analyzed the data from genome sequencing. CH, ML, ID were responsible for initiation and supervision of the study. ID performed the data analysis for phenotyping microarray experiments. PK wrote a MATLAB script for determination of the CO_2 uptake rates. All authors read and approved the final manuscript.

Funding

Financial support was provided by the “Vienna Business Agency”, [ID 1890571, 2017]. Irina Druzhinina was supported by Austrian Science Fund FWF, P25745-B20.

Availability of data and materials

The data sets supporting the conclusions of this article are included in the main article as well as the supplementary data. The raw data would remain confidential and will not be shared due to a filed patent application (No. A68/2018).

Appendix A. Supplementary data

Supplementary data associated with this article can be found, in the online version, at https://doi.org/10.1016/j.biortech.2018.06.057.

References

Akiyama, M., Crooke, E., Kornberg, A., 1993. An exopolyphosphatase of *Escherichia coli*. The enzyme and its ppx gene in a polyphosphate operon. J. Biol. Chem. 268 (1), 633–639.
Bachmann, B.J., 1983. Linkage map of *Escherichia coli* K-12, edition 7. Microbiol. Rev. 47 (2), 180–230.
Balaji, S., Gopi, K., Muthuvelan, B., 2013. A review on production of poly β hydroxybutyrates from cyanobacteria for the production of bio plastics. Algal Res. 2 (3), 278–285.
Burnap, R.L., Hagemann, M., Kaplan, A., 2015. Regulation of CO_2 Concentrating Mechanism in Cyanobacteria. Life 5 (1), 348–371.
Burut-Archanai, S., Eaton-Rye, J.J., Incharoensakdi, A., 2011. Na^+-stimulated phosphate uptake system in *Synechocystis* sp. PCC 6803 with Pst1 as a main transporter. BMC Microbiol. 11 225 225.
Bustin, S.A., 2004. A-Z of quantitative PCR, 1 ed. Intl Univ Line, La Jolla, California.
Cordero, B.F., Obraztsova, I., Couso, I., Leon, R., Vargas, M.A., Rodriguez, H., 2011. Enhancement of lutein production in *Chlorella sorokiniana (Chorophyta)* by improvement of culture conditions and random mutagenesis. Mar. Drugs 9 (9), 1607–1624.
Cox, G.B., Rosenberg, H., Downie, J.A., Silver, S., 1981. Genetic analysis of mutants affected in the Pst inorganic phosphate transport system. J. Bacteriol. 148 (1), 1–9.
de Jaeger, L., Verbeek, R.E., Draaisma, R.B., Martens, D.E., Springer, J., Eggink, G., Wijffels, R.H., 2014. Superior triacylglycerol (TAG) accumulation in starchless mutants of *Scenedesmus obliquus*:(I) mutant generation and characterization. Biotechnol. Biofuels 7 (1), 69.
De Philippis, R., Ena, A., Guastiini, M., Sili, C., Vincenzini, M., 1992. Factors affecting poly-β-hydroxybutyrate accumulation in cyanobacteria and in purple non-sulfur bacteria. FEMS Microbiol. Lett. 103 (2), 187–194.
Diaz-Troya, S., Lopez-Maury, L., Sanchez-Riego, A.M., Roldan, M., Florencio, F.J., 2014. Redox regulation of glycogen biosynthesis in the cyanobacterium *Synechocystis* sp. PCC 6803: analysis of the AGP and glycogen synthases. Mol. Plant 7 (1), 87–100.
Doan, T.T.Y., Obbard, J.P., 2012. Enhanced intracellular lipid in Nannochloropsis sp. via random mutagenesis and flow cytometric cell sorting. Algal Res., 1(1), 17–21.
Drosg, B., 2015. Photo-autotrophic Production of Poly(hydroxyalkanoates) in Cyanobacteria. Chem. Biochem. Eng. Q. 29 (2), 145–156.
Dutt, V., Srivastava, S., 2017. Novel quantitative insights into carbon sources for synthesis of poly hydroxybutyrate in Synechocystis PCC 6803. Photosynthesis Res.
Fabra, M.J., López-Rubio, A., Lagaron, J.M., 2015. Three-Layer Films Based on Wheat Gluten and Electrospun PHA. Food Bioprocess Technol. 8 (11), 2330–2340.
Forchhammer, K., Tandeau de Marsac, N., 1995. Functional analysis of the phosphoprotein PII (glnB gene product) in the cyanobacterium *Synechococcus* sp. strain PCC 7942. J. Bacteriol. 177 (8), 2033–2040.
Galanie, S., Siddiqui, M.S., Smolke, C.D., 2013. Molecular tools for chemical biotechnology. Curr. Opin. Biotechnol. 24 (6). http://dx.doi.org/10.1016/j.copbio.2013.03.001.
Gao, Z., Zhao, H., Li, Z., Tan, X., Lu, X., 2012. Photosynthetic production of ethanol from carbon dioxide in genetically engineered cyanobacteria. Energy Environ. Sci. 5 (12), 9857–9865.
Gomez-Garcia, M.R., Fazeli, F., Grote, A., Grossman, A.R., Bhaya, D., 2013. Role of Polyphosphate in Thermophilic *Synechococcus* sp. from Microbial Mats. J. Bacteriol. 195 (15), 3309–3319.
Hauf, W., Watzer, B., Roos, N., Klotz, A., Forchhammer, K., 2015. Photoautotrophic Polyhydroxybutyrate Granule Formation Is Regulated by Cyanobacterial Phasin PhaP in *Synechocystis* sp. Strain PCC 6803. Appl. Environ. Microbiol. 81 (13), 4411–4422.
Hein, S., Tran, H., Steinbuchel, A., 1998. *Synechocystis* sp. PCC6803 possesses a two-component polyhydroxyalkanoic acid synthase similar to that of anoxygenic purple sulfur bacteria. Arch. Microbiol. 170 (3), 162–170.
Hofer, A., Kamravamanesh, D., Bona-Lovasz, J., Limbeck, A., Lendl, B., Herwig, C., Fricke, J., 2018. Prediction of filamentous process performance attributes by CSL quality assessment using mid-infrared spectroscopy and chemometrics. J. Biotechnol. 265, 93–100.

Kamravamanesh, D., Pflügl, S., Nischkauer, W., Limbeck, A., Lackner, M., Herwig, C., 2017. Photosynthetic poly-β-hydroxybutyrate accumulation in unicellular cyanobacterium Synechocystis sp. PCC 6714. AMB Express, 7(1), 143.
Khetkorn, W., Incharoensakdi, A., Lindblad, P., Jantaro, S., 2016. Enhancement of poly-3-hydroxybutyrate production in *Synechocystis* sp. PCC 6803 by overexpression of its native biosynthetic genes. Bioresour. Technol. 214, 761–768.
Kopf, M., Klähn, S., Voss, B., Stüber, K., Huettel, B., Reinhardt, R., Hess, W.R. 2014. Finished genome sequence of the unicellular cyanobacterium Synechocystis sp. strain PCC 6714. GenomeA, 2(4), e00757–14.
Lackner, M. 2015. Bioplastics. In: Kirk-Othmer Encyclopedia of Chemical Technology. John Wiley & Sons, Inc.
Lau, N.-S., Foong, C.P., Kurihara, Y., Sudesh, K., Matsui, M., 2014. RNA-Seq Analysis Provides Insights for Understanding Photoautotrophic Polyhydroxyalkanoate Production in Recombinant *Synechocystis* sp. PLoS One 9 (1), e86368.
Madison, L.L., Huisman, G.W., 1999. Metabolic Engineering of Poly(3-Hydroxyalkanoates): from DNA to Plastic. Microbiol. Mol. Biol. Rev. 63 (1), 21–53.
Monds, R.D., Silby, M.W., Mahanty, H.K., 2001. Expression of the Pho regulon negatively regulates biofilm formation by *Pseudomonas aureofaciens* PA147-2. Mol. Microbiol. 42 (2), 415–426.
Narusaka, Y., Narusaka, M., Satoh, K., Kobayashi, H., 1999. In vitro random mutagenesis of the D1 protein of the photosystem II reaction center confers phototolerance on the cyanobacterium *Synechocystis* sp. PCC 6803. J. Biol. Chem. 274 (33), 23270–23275.
Nishioka, M., Nakai, K., Miyake, M., Asada, Y., Taya, M., 2001. Production of poly-β-hydroxybutyrate by thermophilic cyanobacterium, *Synechococcus* sp. MA19, under phosphate-limited conditions. Biotechnol. Lett. 23, 1095–1099.
Oliver, N.J., Rabinovitch-Deere, C.A., Carroll, A.L., Nozzi, N.E., Case, A.E., Atsumi, S., 2016. Cyanobacterial metabolic engineering for biofuel and chemical production. Curr. Opin. Chem. Biol. 35, 43–50.
Osanai, T., Azuma, M., Tanaka, K., 2007. Sugar catabolism regulated by light- and nitrogen-status in the cyanobacterium *Synechocystis* sp. PCC 6803. Photochem. Photobiol. Sci. 6 (5), 508–514.
Osanai, T., Kanesaki, Y., Nakano, T., Takahashi, H., Asayama, M., Shirai, M., Kanehisa, M., Suzuki, I., Murata, N., Tanaka, K., 2005. Positive regulation of sugar catabolic pathways in the cyanobacterium *Synechocystis* sp. PCC 6803 by the group 2 sigma factor sigE. J. Biol. Chem. 280 (35), 30653–30659.
Pietrini, M., Roes, L., Patel, M.K., Chiellini, E., 2007. Comparative life cycle studies on poly(3-hydroxybutyrate)-based composites as potential replacement for conventional petrochemical plastics. Biomacromolecules 8 (7), 2210–2218.
Pinzari, F., Ceci, A., Abu-Samra, N., Canfora, L., Maggi, O., Persiani, A., 2016. Phenotype MicroArray™ system in the study of fungal functional diversity and catabolic versatility. Res. Microbiol. 167 (9), 710–722.
Rao, N.N., Gómez-García, M.R., Kornberg, A., 2009. Inorganic Polyphosphate: Essential for Growth and Survival. Annu. Rev. Biochem. 78 (1), 605–647.
Rao, N.N., Torriani, A., 1990. Molecular aspects of phosphate transport in *Escherichia coli*. Mol. Microbiol. 4 (7), 1083–1090.
Rippka, R., Deruelles, J., Waterbury, J.B., Herdman, M., Stanier, R.Y., 1979. Generic assignments, strain histories and properties of pure cultures of cyanobacteria. Microbiology 111 (1), 1–61.
Ruffing, A.M., Kallas, T., 2016. Editorial: Cyanobacteria: the Green E. coli. Front. Bioeng. Biotechnol. 4, 7.
Schlebusch, M., Forchhammer, K., 2010. Requirement of the nitrogen starvation-induced protein Sll0783 for polyhydroxybutyrate accumulation in *Synechocystis* sp. strain PCC 6803. Appl. Environ. Microbiol. 76 (18), 6101–6107.
Sudesh, K., Taguchi, K., Doi, Y., 2002. Effect of increased PHA synthase activity on polyhydroxyalkanoates biosynthesis in *Synechocystis* sp. PCC6803. Int. J. Biol. Macromol. 30 (2), 97–104.
Surin, B.P., Rosenberg, H., Cox, G.B., 1985. Phosphate-specific transport system of *Escherichia coli*: nucleotide sequence and gene-polypeptide relationships. J. Bacteriol. 161 (1), 189–198.
Suzuki, E., Ohkawa, H., Moriya, K., Matsubara, T., Nagaike, Y., Iwasaki, I., Fujiwara, S., Tsuzuki, M., Nakamura, Y., 2010. Carbohydrate metabolism in mutants of the cyanobacterium *Synechococcus elongatus* PCC 7942 defective in glycogen synthesis. Appl. Environ. Microbiol. 76 (10), 3153–3159.
Taroncher-Oldenburg, G., Nishina, K., Stephanopoulos, G., 2000. Identification and analysis of the polyhydroxyalkanoate-specific β-ketothiolase and acetoacetyl coenzyme A reductase genes in the cyanobacterium *Synechocystis* sp. strain PCC6803. Appl. Environ. Microbiol. 66 (10), 4440–4448.
Vuppada, R.K., Hansen, C.R., Strickland, K.A.P., Kelly, K.M., McCleary, W.R., 2018. Phosphate signaling through alternate conformations of the PstSCAB phosphate transporter. BMC Microbiol. 18 (1), 8.
Wang, B., Pugh, S., Nielsen, D.R., Zhang, W., Meldrum, D.R., 2013. Engineering cyanobacteria for photosynthetic production of 3-hydroxybutyrate directly from CO_2. Metab. Eng. 16, 68–77.
Wang, C., Kim, J.-H., Kim, S.-W., 2014. Synthetic Biology and Metabolic Engineering for Marine Carotenoids: New Opportunities and Future Prospects. Mar. Drugs 12 (9), 4810.
Xu, Y., Tiago Guerra, L., Li, Z., Ludwig, M., Charles Dismukes, G., Bryant, D.A., 2013. Altered carbohydrate metabolism in glycogen synthase mutants of *Synechococcus* sp. strain PCC 7002: Cell factories for soluble sugars. Metab. Eng. 16, 56–67.